

Design and application of a high-temperature microfurnace for an *in situ* X-ray diffraction study of phase transformation

W. S. Eu, W. H. Cheung and M. Valix*

School of Chemical and Biomolecular Engineering, The University of Sydney, Sydney, Australia.
E-mail: mvalix@usyd.edu.au

Thermal treatment of mineral ores such as ilmenite can initiate phase transformations that could affect their activation or deactivation, subsequently influencing their ability to dissolve in a leaching agent. Most laboratory-based X-ray diffraction (XRD) studies were carried out *ex situ* in which realistic diffraction patterns could not be obtained simultaneously with occurring reactions and were time-consuming. The availability of synchrotron-radiation-based XRD not only allows *in situ* analysis, but significantly shortens the data recording time. The present study details the design of a robust high-temperature microfurnace which allows thermal processing of mineral ore samples and the simultaneous collection of high-resolution synchrotron XRD data. In addition, the application of the manufactured microfurnace for *in situ* study of phase transformations of ilmenite ore under reducing conditions is demonstrated.

© 2009 International Union of Crystallography
Printed in Singapore – all rights reserved

Keywords: furnace; *in situ* X-ray diffraction; ilmenite; phase transformation.

1. Introduction

X-ray diffraction (XRD) is a widely applied technique for identifying crystalline phases in material samples (Sparks, 1998). It has been used to study crystalline phases in heterogeneous catalysts (Chupas *et al.*, 2001; Clausen *et al.*, 1991) and recently extended to include the broader spectrum of solid state chemistry, such as solid state reactions, phase transformations, crystallite growth and thermal expansion of metal compounds (Dapiaggi *et al.*, 2002; Kim *et al.*, 2003, 2004; Rodriguez *et al.*, 2002; Wang *et al.*, 2004). X-ray diffraction can also be used as an adjunct tool to conventional thermal analytical methods such as thermogravimetry and differential scanning calorimetry, allowing effective identification of phase transformations, texture analysis and crystallite size measurements (Dapiaggi *et al.*, 2002).

In general, conventional XRD studies are performed *ex situ* using laboratory-based low-energy copper, cobalt (O'Connor *et al.*, 2004) or molybdenum sources (Sparks, 1998). Solid samples are removed from the reactor and analysed after exposure to ambient conditions. As a result, ideal XRD patterns cannot be obtained simultaneously with ideal chemical activity measurements in real time without altering the sample (Clausen *et al.*, 1991). Furthermore, low-energy X-ray sources with fixed wavelengths are unable to generate high-resolution patterns for accurate measurement of crystal

cell parameters nor identification of trace compounds, owing to the relatively high background noise.

In situ XRD under non-ambient conditions is one of the best methods of studying dynamic processes in solid crystalline samples (Dapiaggi *et al.*, 2002), permitting real-time XRD measurements while physical changes or chemical reactions are taking place. For this purpose, high-energy synchrotron-radiation-based X-ray diffraction is preferred as it provides broad tunable energy spectra which are sufficiently robust for energy scanning experiments (Valix & Cheung, 2002). Synchrotron radiation of considerably higher energy can better penetrate solid samples to minimize absorption effects. These characteristics are particularly desirable in performing fast real-time measurements to give high-resolution data and bulk analysis of the sample without negating the kinetic effects of the reacting sample.

On the other hand, thermal activation of oxide ores has been shown to enhance the hydrometallurgical reactivity of minerals (Nguyen, 2005). The enhanced reactivity resulting from 'thermal activation' is associated with improvement of textural properties (*e.g.* surface area), surface reactivity and mineralogical transformations. Owing to the complex composition of oxide ores, the thermal activation process involves a series of dynamic solid state reactions, which are difficult to capture by the *ex situ* analysis. Accurate interpretations of mineralogical transformations are hindered by

Table 1Comparison of furnace designs for *in situ* synchrotron XRD analysis of solid–gas reactions.

Furnace design	Drawbacks
Clausen <i>et al.</i> (1991)	Quartz/glass capillaries crack easily with the use of hard stainless steel fittings, resulting in gas leakage. The use of a separate gas stream to cool/heat the sample bed externally introduces gas into the evacuated synchrotron diffractometer chamber. The presence of gas may present interference with XRD signals, resulting in lower-resolution data. The use of Kapton foil as a heat shield is complicated and presents difficulties during device set-up. Limited temperature range. Not capable of achieving higher temperatures of interest.
Puxley <i>et al.</i> (1994)	The sample's flat disc set-up introduces Bragg–Brentano geometry which causes potential geometrical aberrations as the sample surface deviates from the focusing plane during heating. Thermal expansion incurs a shift in sample height which must be accounted for during analysis (Margulies <i>et al.</i> , 1999). XRD of a sample in a flat disc set-up is limited to surface analysis which potentially introduces artefacts owing to surface effects. The use of a graphite foil between the hemispheres to minimize convective heat loss reduces X-ray diffraction signals by a quarter (Puxley <i>et al.</i> , 1994). Cell design tailored for use with conventional low-energy diffractometer. Its detailed set-up is not sufficiently portable or compact for synchrotron application with limited beam time allocation.
Margulies <i>et al.</i> (1999)	For inexperienced users, the use of a 3 mm hole and slit cut on the furnace sleeve for X-ray transmission causes potential misalignment of the incident beam with the sample during measurement. This usually results in the detection of negligible signal owing to obstruction or interference of sample diffraction pattern by signals diffracted off the furnace sleeve materials. BeO sample chamber forms a pressurized closed system. An open system is required to better mimic a continuous solid–gas reaction as in actual plug-flow or fluidized bed reactor. Water-cooled fittings introduce potential electrical hazards owing to water leakage. Furnace design is relatively complicated. A simpler furnace design with fewer parts is required for robustness in synchrotron XRD application.
Chupas <i>et al.</i> (2001)	Furnace set-up requires careful insertion and proper positioning of the thermocouple into the sapphire capillary. This will be critical with a limited beam time available. Introduction of thermocouple into the capillary tube also causes a significant pressure drop in gas flow and potential interference to the sample diffraction pattern caused by misalignment during measurement. Thin thermocouples are expensive and have a short life-span which may require frequent replacement. Sample bed cannot achieve uniform heating using only one heating wire placed parallel to capillary surface. From our trials, heating wires easily buckle off capillary surface owing to thermal expansion resulting in reduced thermal contact. Furnace is difficult to set up with the use of an alumina heat shield as it requires effort to carefully align the sample with the incident beam.

problems such as rapid intermediate reactions and reversibility of phase transformation upon exposure to ambient conditions (Valix & Cheung, 2002).

In order to study the phase transformation of mineral ores *in situ* during thermal treatment, it is necessary to construct a microfurnace that is capable of heating to desired temperatures, and supports a reactor which allows for solid–gas reactions to take place and accurately positions the sample for synchrotron-radiation-based XRD analysis. Several furnace designs have been considered from previous studies (Brand & Goldschmidt, 1956; Klug & Alexander, 1974; Puxley *et al.*, 1994; Vries, 1978). However, most of the designs are not suitable for the present study because they have been specifically designed for applications using low-energy laboratory-based XRD. In particular, furnaces with a plate-type sample holder constitute the Bragg–Brentano geometry which introduces geometrical aberrations as the surface of a flat sample deviates from the focusing plane. This is because the height of the sample changes as it is heated. To account for this error, the sample height must be calibrated for different sample materials, temperatures and heating rates, and regimes which complicate analysis (Margulies *et al.*, 1999). Furthermore, the plate-type sample holder suffers significant mass transfer effects as reacting gases are passed over the sample surface, rather than through the sample bed, causing a reduced extent of reaction (Puxley *et al.*, 1994). Hence, the Debye–Scherrer geometry is preferred for the *in situ* high-temperature XRD

analysis to alleviate these complications. However, newer furnace designs for the synchrotron-radiation-based XRD (Chupas *et al.*, 2001; Clausen *et al.*, 1991; Dapiaggi *et al.*, 2002; Kim *et al.*, 2003, 2004; Margulies *et al.*, 1999; Puxley *et al.*, 1994; Wang *et al.*, 2004) are not sufficiently robust and present several drawbacks during XRD data collection. A comparison of selected earlier furnace designs which support solid–gas reactions for synchrotron XRD analysis are shown in Table 1.

Hence, a new microfurnace was designed specifically for the *in situ* study of phase transformations during thermal treatment of mineral ore under simulated reaction conditions at temperatures up to 1123 K, by incorporating the best features of earlier furnace designs. This paper specifically details the design of the microfurnace and experimental set-up for the synchrotron radiation X-ray powder diffraction technique. Preliminary results of the mineral phase transformation of ilmenite mineral ore samples undergoing reduction will be used to illustrate the workability of the microfurnace design.

2. Materials and methods

2.1. Microfurnace

The high-temperature microfurnace (Fig. 1) is designed based on five main considerations: (i) provision for solid–gas reactions, (ii) operating temperature range, (iii) temperature uniformity, (iv) sample positioning in a Debye–Scherrer

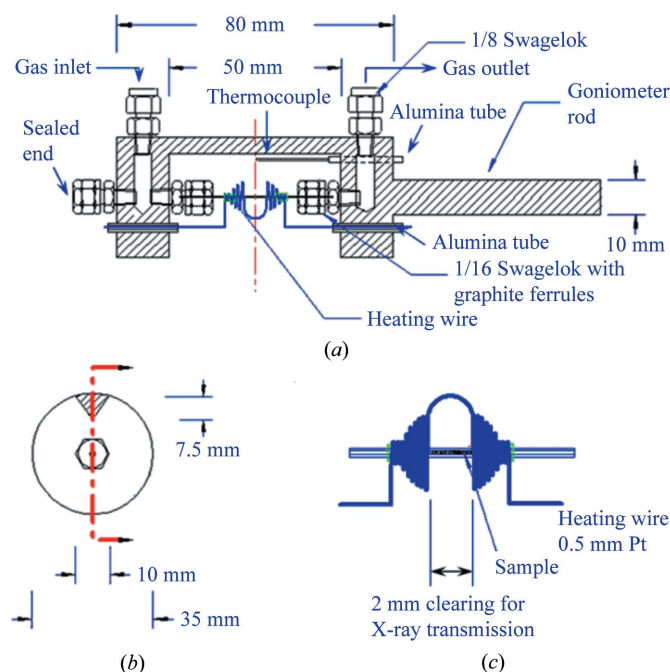


Figure 1 Schematic diagram (not to scale) showing the continuous-flow micro-furnace design. (a) Cross-sectional view. (b) Front view. (c) Capillary tube details.

diffractometer and (v) robustness during changeover in between test runs. The microfurnace consists of two primary parts, namely the furnace frame and the heating element.

The primary purpose of the microfurnace frame is to support the reactor and the heating element and to provide an open channel for the continuous gas flow through the reactor. The reactor consists of an open-ended quartz capillary of 0.7 mm outer diameter (OD) and 0.01 mm wall thickness. Powdered mineral sample is loaded into the capillary between two pieces of kaowool to fix the position of the sample bed while reactant gas is passed through it. The pre-loaded capillary is firmly mounted onto the furnace frame using 1/16" stainless steel leak-free fittings with graphite ferrules. The furnace frame is connected to a gas input and exhaust using 1/8" stainless steel leak-free fittings (see Fig. 1a). The mounting of the capillary is relatively simple but caution is needed to avoid over-tightening the leak-free fittings. One end of the furnace consists of a 10 mm OD rod which could be attached firmly onto the goniometer of the diffractometer. This allows for accurate positioning of the reactor in the path of the X-ray transmission and allows for 2θ rotation with the remotely controlled rotor during the XRD analysis. The supporting beam of the furnace is tapered (see Fig. 1b) to maximize the free space for unobstructed X-ray transmission. The furnace can be rocked up to a maximum of 270° during XRD measurement to minimize effects of preferred orientation.

The angular resolution of the XRD pattern is essentially determined by the outer diameter of the capillary tube and the distance of the sample bed from the detector (Clausen *et al.*, 1991). Using highly crystalline silicon as the calibrant sample

in a 0.7 mm OD quartz capillary aligned within the incident beam of fixed wavelength 1 \AA , the typical systematic error is recorded at approximately $\Delta 2\theta = 0.0900^\circ$.

The sample bed is heated by an external platinum–30%–rhodium heating element, which is capable of achieving high temperatures (up to a maximum of 1273 K) within a limited space. This material is exceptionally resistant to oxidation, has a sufficiently high melting point and good mechanical properties in the desired temperature range. The heating wire is coiled around the capillary reactor in the shape of two hemispheres separated by a 2 mm-wide gap (see Fig. 1c). The unique shape of the heating wire allows uniform radiative heating of the entire sample bed without the need for an additional heat shield as reported in other designs (Chupas *et al.*, 2001; Clausen *et al.*, 1991; Margulies *et al.*, 1999). This is because the use of an aluminium heat shield to maintain temperature uniformity (Chupas *et al.*, 2001) often causes interference to the X-ray diffraction signals, which adds on to the sample diffraction pattern. Temperature uniformity along the axial distance of the heating coil has been tested using a Leeds & Northrop hot wire pyrometer. The pyrometer is aligned such that the hot wire ran along the length of the quartz sample tube, which is then placed at a series of points along the heating coil axis. The temperature of the hot wire is then adjusted until it disintegrates and disappears. This is recorded as the temperature attainable for the particular current input. The heating coiling is then adjusted to give the most uniform temperature distribution. This is to achieve no discernible temperature difference (within $\pm 5 \text{ K}$) over the length of the tube located within the path of the X-ray transmission, which corresponds to the 2 mm gap of the heating coil.

The use of a resistive heating wire also negates the use of pre-heated air as the heat source as seen in a previous design (Clausen *et al.*, 1991), which introduced heated air into the vacuum diffractometer chamber. The presence of air is undesirable as it interferes with the signal resolution and the furnace's heating regime. The ends of the heating wire are embedded in alumina tubes to insulate the furnace frame against the electrical current and heat. The temperature of the sample bed is monitored using a 1 mm type-K thermocouple; its tip is suspended above the sample bed (see Fig. 1a) without interfering with the X-ray beam. The heating wire is powered by a 16 A power supply and the temperature is controlled to within 2 K by regulating its current supply. However, this would result in an offset of temperature inside the sample bed (actual temperature) with the temperature measured by the thermocouple. Regular temperature calibration is needed to ensure that the temperature is within the experimental requirement.

The overall dimensions of the furnace are 150 mm (L) \times 40 mm (W), and it only weighs 200 g which provides ease of portability (particularly for travel to international beamline facilities). Fig. 2 shows a photograph of the completed microfurnace attached to the goniometer of the synchrotron diffractometer.

Table 2
Chemical analysis (wt%) of Australian ilmenite ore (by X-ray fluorescence).

TiO ₂	FeO	Fe ₂ O ₃	MnO	SiO ₂	Al ₂ O ₃	V ₂ O ₅	MgO	CaO	Others
63.7	2.9	25.8	1.02	1.13	1.5	0.15	0.19	0.03	3.58%

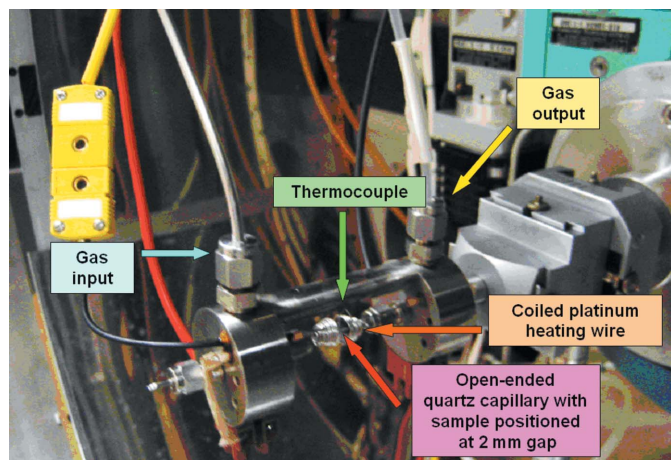


Figure 2
Photograph of the microfurnace.

2.2. Gas flow apparatus

A portable and compact gas flow apparatus is designed to deliver reacting gases to the capillary reactor in the X-ray diffractometer chamber safely and to meet experiment requirements. Fig. 3 shows a schematic diagram of the gas flow apparatus set-up detailing this arrangement.

For the ilmenite reduction study, hydrogen gas is supplied to the reactor in the form of a pre-mixed gas (4% hydrogen and 96% nitrogen) below its lower explosion limit (Australian Standards, 1992). The pre-mixed gas is used as the reducing agent for the ilmenite mineral samples undergoing thermal processing. Nitrogen gas is supplied separately to purge the system of air (and oxygen) prior to the commencement of the reduction tests. The required amount of pre-mixed and nitrogen gases are metered into the reactor using corresponding rotameters. Non-return valves are used to prevent the backflow of gas from the reactor to the gas cylinders in the case of low cylinder pressure or flashback. This feature is an important precaution against potential fire or explosion hazards owing to gas cylinder failure. In general, the present furnace design can be adapted to other gases with ease.

As the *in situ* tests take place in an enclosed diffractometer chamber, a differential pressure gauge is installed across the reactor at the gas inlet and outlet to determine the presence of gas flow through the capillary reactor. Excessive pressure drop might indicate

a broken capillary or gas leakage in the process line during the *in situ* tests. The gas inlet and outlet are connected to the reactor in the diffractometer through a custom-made back plate with leak-free fittings. Nylon tubing is used for its flexibility in the confined space. A flashback arrestor is installed downstream of the gas flow apparatus as a precaution against the risk of flashback into the diffractometer. In addition, a hydrogen detector is placed in the hutch, above the diffractometer, to detect potential hydrogen gas leakage from the gas lines and fittings. The hydrogen detector is relayed to a solenoid valve (V-3) at the output of the hydrogen gas cylinder. In cases when hydrogen exceeds the safety limit, the solenoid valve would be automatically shut off.

2.3. Materials

The ore tested in this study is a weathered Australian ilmenite ore. The X-ray fluorescence chemical analysis of this ore is shown in Table 2.

Pure alpha-phase alumina (Al₂O₃) from Sigma Aldrich was used as a temperature calibrant. A pre-mixed gas (4% hydrogen and 96% nitrogen) was used as the reducing agent for the ilmenite reduction tests.

2.4. *In situ* temperature-resolved reduction tests

Temperature-resolved *in situ* ilmenite reduction tests were conducted at the Australian National Beamline Facility (ANBF), beamline BL-20B of the Photon Factory, Tsukuba, Japan. Finely powdered ilmenite sample was packed into a 0.7 mm OD quartz capillary reactor, which was then mounted

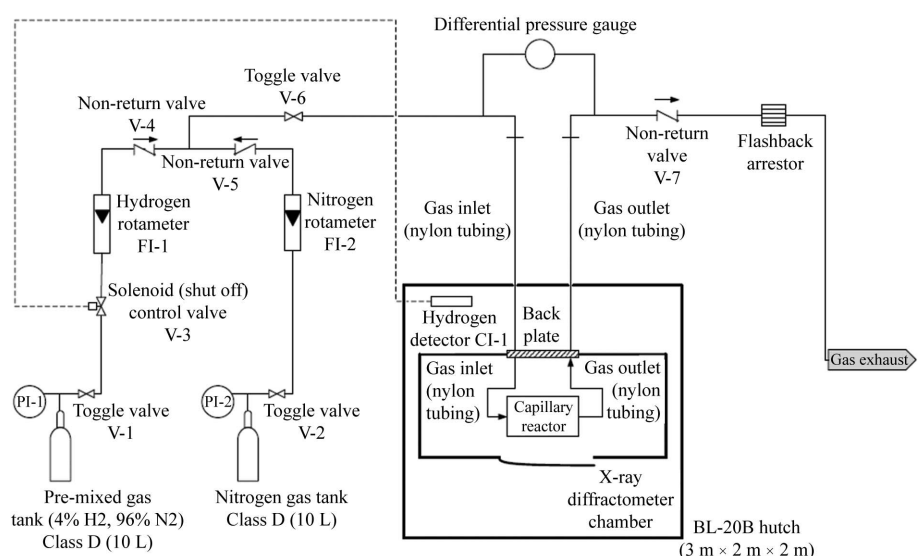


Figure 3
Schematic diagram showing the set-up of the gas flow apparatus.

onto the microfurnace. The sample bed in the capillary reactor was aligned in the path of the X-ray beam using the goniometer. A pre-mixed gas (4% hydrogen and 96% nitrogen) was supplied in continuous flow to the capillary reactor using the gas flow apparatus. The temperature range 298–1123 K was investigated. The diffraction signals were obtained with X-rays of fixed wavelength, $\lambda = 1.0 \text{ \AA}$, at a 2θ scanning rate of 1° min^{-1} in the evacuated diffractometer chamber with a gauge pressure of 1 torr (133 Pa). The diffracted X-ray signals were collected using image plates as detector in which data were extracted using the Fuji BAStation image-plate reader.

The use of an open-ended quartz capillary in the *in situ* tests involving solid–gas reactions mimics the continuous ilmenite ore reduction process carried out in the laboratory pilot reactor under similar conditions. As such, this allows a more consistent comparison between *in situ* and *ex situ* test results.

3. Results and discussion

3.1. Temperature calibration

In order to determine the temperature profile along the axis of the heating coil, a separate 1 mm type-K thermocouple was inserted into the furnace through the heating coil in place of the capillary tube. The furnace temperature was set at 543 K for this test. The temperatures along the axial distance of the heating coil were measured at intervals of 1 mm when steady state was achieved. Twenty readings were taken at each axis point. Fig. 4 shows the axial thermal gradient profile of the heating coil. Point 0 corresponds to the centre of the coil gap where the sample was accurately aligned with the 2 mm (horizontal) \times 1 mm (vertical) incident X-ray beam. Although results showed that the measured temperatures generally deviate from the coil centre, the measured temperature at the sample position remained consistent with a standard deviation of 5 K, as expected from earlier furnace trials. This temperature profile is not expected to affect the effective sample temperature because XRD measurements will be taken at the exact sample position each time. Also, this test was carried out under convective conditions (room atmosphere) where the

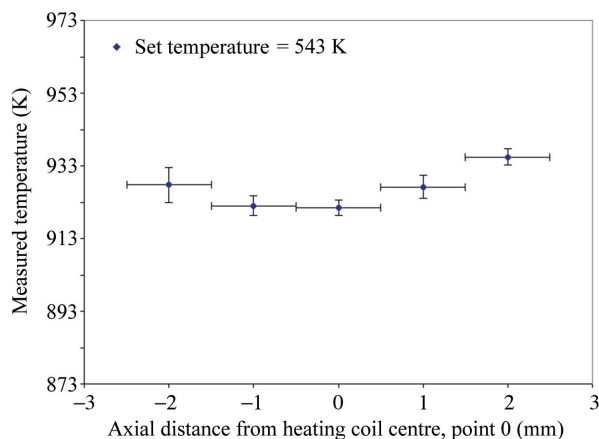


Figure 4
Heating coil axial thermal gradient profile.

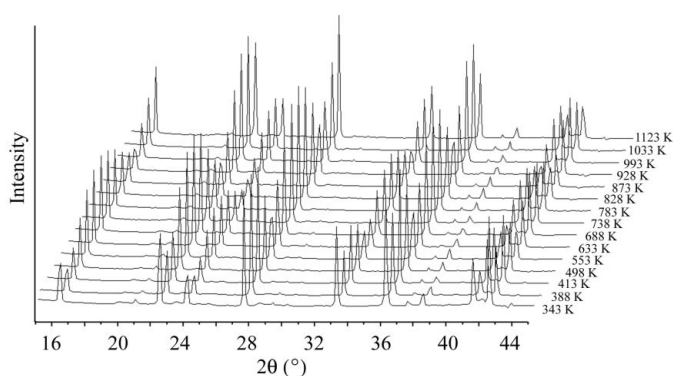


Figure 5
Plots of *in situ* temperature-resolved XRD patterns of $\alpha\text{-Al}_2\text{O}_3$ temperature calibrant undergoing thermal lattice expansion.

error in temperature measurements is more prominent compared with actual *in situ* XRD measurements, which are carried out under radiative conditions (under 1 torr vacuum) (Brand & Goldschmidt, 1956).

Temperature calibration was performed to determine the relationship between the measured and the actual temperatures of the sample bed. The calibration was carried out by means of the known thermal expansion of a standard material (alpha-phase alumina, $\alpha\text{-Al}_2\text{O}_3$, was used for this purpose) under conditions similar to those of actual *in situ* XRD tests. The temperature of the microfurnace was ramped at a constant maximum heating rate from room temperature to a measured temperature of 583 K with a step size of 20 K. Each temperature was held for 10 min. Diffraction signals from heated alpha-alumina were obtained with fixed X-rays of wavelength $\lambda = 1.0 \text{ \AA}$ using image plates as detector in a vacuum with a gauge pressure of 1 torr (133 Pa). Fig. 5 shows a typical temperature-resolved XRD pattern of $\alpha\text{-Al}_2\text{O}_3$ calibrant undergoing thermal lattice expansion.

The X-ray diffraction profiles of the alpha-alumina heated at each temperature were then refined by the Rietveld method using the *General Structure Analysis System (GSAS)* and *EXPGUI* software (Larson & Von Dreele, 1994; Toby, 2001) to obtain the corresponding unit-cell parameters. These unit-cell parameter data were correlated against literature values (Swenson *et al.*, 1985; Dapiaggi *et al.*, 2002) to determine the actual temperatures.

Fig. 6 shows the resulting temperature calibration chart for the microfurnace by means of the thermal expansion of the alpha-phase alumina. Results suggest that the microfurnace is capable of achieving high temperatures (up to 1123 K for ilmenite reduction). This has been verified by *ex situ* temperature measurement using a below-red pyrometer at similar power supply settings. The linear relationship between the measured and actual temperatures allows easy data interpolation for calculating the temperature of interest. However, it must be noted that the calibration curve is not reproducible, as suggested by the significant standard deviation based on furnace calibrations conducted at a separate synchrotron beam session. Precaution is taken by recalibrating the furnace each time prior to the execution of *in situ* tests and

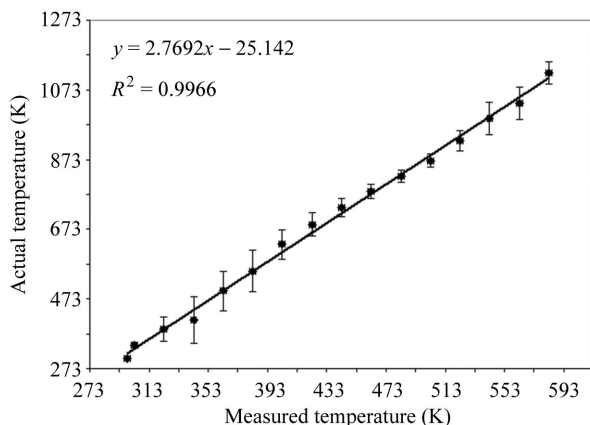


Figure 6
Calibration of sample temperatures.

by spiking samples with a known weight percentage of alpha-alumina calibrant. A reliable literature value of the alpha-alumina thermal lattice expansion (Swenson *et al.*, 1985, Dapiaggi *et al.*, 2002) is essential to attain accurate actual temperature measurements.

3.2. Example: phase transformation of ilmenite during reduction

Fig. 7 shows typical *in situ* XRD patterns of an Australian ilmenite mineral sample (with 50 wt% alpha-alumina internal standard) undergoing reduction at increasing temperatures.

The 2θ values of each set of XRD patterns were matched against the International Centre for Diffraction Data (ICDD) to identify the mineral phases which were present at any one stage of the reduction process. The formation and decomposition of mineral phases can then be used to derive an understanding of the solid state reactions and the mechanisms involved in the ilmenite reduction process.

Upon identification, the relative intensities of specific mineral phases can then be plotted against reduction temperatures. As an example, Fig. 8 shows the change in the relative intensities of diffraction peaks for ferric pseudobrookite and ferrous-pseudobrookite mineral phases as the ilmenite sample is reduced at increasing temperatures. Other mineral phases were omitted as they show no significant changes in intensities during reduction.

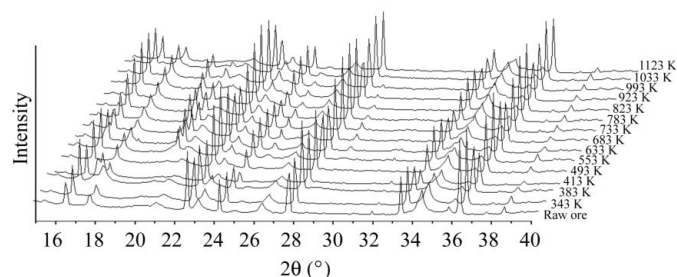


Figure 7
Plots of the *in situ* XRD patterns of an Australian ilmenite mineral (with 50 wt% alpha-alumina internal standard) undergoing reduction at increasing temperatures.

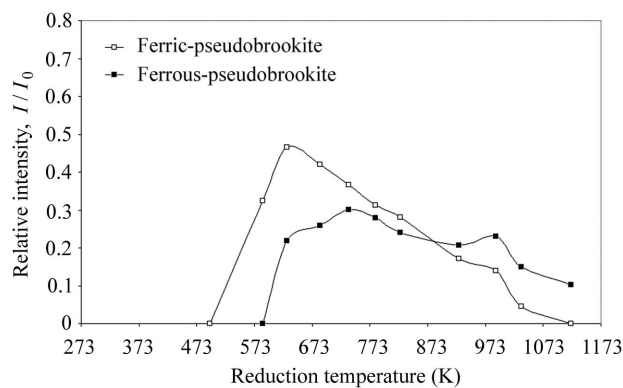


Figure 8
Phase transformation of Australian ilmenite ore undergoing reduction.

As shown, ferric pseudobrookite formed at 573 K. Its intensity peaked at 623 K but declined gradually at higher temperatures as it gradually transformed into ferrous-pseudobrookite. At temperatures above 773 K the ferrous-pseudobrookite intensity continued to decline with temperature. This transformation was not observed for the *ex situ* measurement. The presence of ferrous-pseudobrookite is associated with an increase in titanium and iron recovery from ilmenite ore (Eu *et al.*, 2008). This result indicates that weathered ilmenite mineral can be activated by reduction. A more detailed study of the titanium and iron recovery is being carried out and will be the subject of future publications.

3.3. Limitations of the present furnace design

As discussed in the previous sections, the present furnace is capable of achieving its design criteria. It provides ease in setting up and transportation, is adaptable and robust, and has few parts. However, it does have its drawbacks. These include (i) temperature calibration at each beam session, (ii) a rotation limit, up to 270°, (iii) a stable temperature zone of 4 mm. Overall, this furnace is compact and simple to set up, and works for most solid–gas reactions.

4. Conclusion

The design of a compact and robust microfurnace for a capillary reactor has enabled *in situ* X-ray diffraction analysis of ilmenite mineral phase transformations during reduction. The microfurnace's unique hemispherical Pt–30%Rh heating element allows rapid and uniform heating of the entire sample bed to sufficiently high temperatures which minimizes mass transfer effects; this is essentially important for kinetic studies of solid state chemistry. The wide temperature range of the microfurnace provides the flexibility required to study the ilmenite reduction at temperatures of interest. It is recommended that temperature calibration be performed for the microfurnace prior to each synchrotron beam session to ensure accurate temperature measurements. The microfurnace frame is custom-made to allow rotation of the sample bed with the goniometer during XRD analysis in order to give a more representative bulk study of the sample bed, hence

reducing the effects of preferred orientation. Open-ended capillary tubes also mimic the continuous solid–gas reactions in *ex situ* pilot ilmenite reduction plants. This allows a more consistent comparison between the *in situ* and *ex situ* analyses. The workability of the microfurnace has been demonstrated in a study of the dynamic chemistry of a mineral extraction system, namely ilmenite reduction. The structural changes observed from the Bragg diffraction patterns formed at various reduction temperatures are used to derive an understanding of the mechanisms involved in the ilmenite reduction process. Preliminary results show that the activation of weathered Australian ilmenite ore is achievable by reduction.

This work was performed at the Australian National Beamline Facility with support from the Australian Synchrotron Research Program, which is funded by the Australian Federal Government's Major National Research Facilities program and the National Collaborative Research Infrastructure Scheme. The authors would like to thank Dr Garry Foran and Dr James Hester of ANBF for their assistance in setting up the experiment. In particular, the authors would like to extend their immense gratitude to Mr Philip Grazier and his team at BHP Billiton for the valuable discussion in designing and constructing the microfurnace. The authors are also grateful to BHP Billiton for providing the ilmenite ore samples. One of the authors (WSE) would like to acknowledge support from the Endeavour International Postgraduate Research Scholarship granted by the Australian Department of Education, Science and Training and the International Postgraduate Award granted by the University of Sydney.

References

Australian Standards (1992). Australian Standard 2508.2.002.

- Brand, J. A. & Goldschmidt, H. J. (1956). *J. Sci. Instrum.* **33**, 41–45.
- Chupas, P. J., Ciraolo, M. F., Hanson, J. C. & Grey, C. P. (2001). *J. Am. Chem. Soc.* **123**, 1694–1702.
- Clausen, B. S., Steffensen, G., Fabius, B., Villadsen, J., Feidenhans'l, R. & Topsoe, H. (1991). *J. Catal.* **132**, 524–535.
- Dapiaggi, M., Artioli, G. & Petras, L. (2002). *Rigaku J.* **19**, 35–41.
- Eu, W. S., Valix, M. & Cheung, W. H. (2008). *XXIV International Mineral Processing Congress*, Beijing, China.
- Kim, J. Y., Hanson, J. C., Frenkel, A. I., Lee, P. L. & Rodriguez, J. A. (2004). *J. Phys. Condens. Matter*, **16**, 3479–3484.
- Kim, J. Y., Rodriguez, J. A., Hanson, J. C., Frenkel, A. I. & Lee, P. L. (2003). *J. Am. Chem. Soc.* **125**, 10684–10692.
- Klug, H. P. & Alexander, L. E. (1974). *X-ray Diffraction Procedures for Polycrystalline and Amorphous Materials*, 2nd ed. New York: John Wiley and Sons.
- Larson, A. C. & Von Dreele, R. B. (1994). *GSAS*, Report LAUR 86-748. Los Alamos National Laboratory, New Mexico, USA.
- Margulies, L., Kramer, M. J., McCallum, R. W., Kycia, S., Haefner, D. R., Lang, J. C. & Goldman, A. I. (1999). *Rev. Sci. Instrum.* **70**, 3554–3561.
- Nguyen, H. B. (2005). Undergraduate thesis, The University of Sydney, Australia.
- O'Connor, F., Cheung, W. H. & Valix, M. (2004). *Int. J. Miner. Process.* **80**, 88–99.
- Puxley, D. C., Squire, G. D. & Bates, D. R. (1994). *J. Appl. Cryst.* **27**, 585–594.
- Rodriguez, J. A., Hanson, J. C., Frenkel, A. I., Kim, J. Y. & Perez, M. (2002). *J. Am. Chem. Soc.* **124**, 346–354.
- Sparks, R. A. (1998). *X-ray Technology, Kirk-Othmer Encyclopedia of Chemical Technology*. New York: John Wiley and Sons.
- Swenson, C. A., Roberts, R. B. & White, G. K. (1985). *Thermal Expansion of Cu, Si, W and Al₂O₃*. Report 590366-757X, pp. 13–19.
- Toby, B. H. (2001). *J. Appl. Cryst.* **34**, 210–213.
- Valix, M. & Cheung, W. H. (2002). *Miner. Eng.* **15**, 607–612.
- Vries, J. L. de (1978). *X-ray Diffraction Review of Literature: Analytical Equipment*, 8th ed. Philips X-ray Diffraction Bulletins, Eindhoven, The Netherlands.
- Wang, X., Hanson, J. C., Frenkel, A. I., Kim, J.-Y. & Rodriguez, J. A. (2004). *J. Phys. Chem. B*, **108**, 13667–13673.